Surface and magnetic interaction effects in Mn_3O_4 nanoparticles

E. Winkler and R. D. Zysler*
Centro Atómico Bariloche, 8400 S.C. de Bariloche, RN, Argentina

D. Fiorani
Istituto di Struttura della Materia-CNR, Area della Ricerca di Roma, C.P. 10, I-00016 Monterotondo, Rome, Italy
(Received 14 April 2004; revised manuscript received 1 July 2004; published 5 November 2004)

The magnetic properties of 15 nm Mn_3O_4 particles, in powder form and dispersed in a polymer at different concentrations (17.6%, 1.5%), have been investigated by magnetization and ESR measurements. Below the ferrimagnetic transition temperature (T_c=42 K), marked differences are observed among the three samples in the temperature dependence of the magnetization, hysteresis loop shape and type and intensity of ESR spectra. They are due to different strengths of interparticle interactions and different contributions from free spins (and free cluster spins) at the particle surface. With decreasing temperature their thermal fluctuations slow down and spins freeze in random directions, according to their local atomic environment. Their fraction is found to decrease with increasing inter-particle interactions, i.e. going from the more diluted particle dispersion to the powder sample.

DOI: 10.1103/PhysRevB.70.174406 PACS number(s): 75.50.Tt, 75.75.+a, 75.50.Gg, 76.50.+g

I. INTRODUCTION

Nanostructured materials are very interesting for the wide range of new physical properties that they exhibit as well as for their applications in different fields (e.g., magnetorecording, permanent magnets, sensors, biomedicine, etc.).[1–3] Due to finite size effects, some basic magnetic properties of materials, e.g., the spontaneous magnetization, the Curie temperature, and the anisotropy energy, are strongly influenced by the particle size. As the particle size decreases, an increasing fraction of atoms lies at or near the surface and then surface and interface effects become more and more important. Because of the presence of defects, missing bonds, fluctuations in number of atomic neighbors and inter-atomic distances, the surface is characterized by topological and magnetic disorder. Such disorder propagates from the surface to the particle core, actually making no longer valid the picture of the particle as a perfectly ordered single domain, whose spins rotate in a synchronous way as a large single spin.[4–10] The resulting magnetic behavior of very small particles is complex and the effect of the interplay of some surface related phenomena is not well understood yet: surface anisotropy, which can give a dominant contribution to the total particle anisotropy, core-surface exchange interaction (exchange anisotropy, in the case of different magnetic phases) and possible competition between surface and core effects.

We have carried out an investigation of the magnetic properties of 15 nm Mn_3O_4 nanoparticles, in powder form and dispersed in a polymer at different concentrations, is reported. Mn_3O_4 (hausmannite) is a material used as catalyst in several chemical reactions (e.g., as the selective reduction of nitrobenzene) and in the manufacture of soft magnetic materials such as the manganese zinc ferrite.[11] The structure of the bulk Mn_3O_4, below 1443 K, is a tetragonal distorted spinel ferrimagnetically ordered below T_c=42 K.[12–16] The comparison of the results of magnetization and electron spin resonance (ESR) provides an evidence that the role of the effective disordered particle surface layer decreases with increasing interparticle interactions (i.e., going from the more diluted particle dispersion to the powder), as shown by the decrease of the fraction of free spins that thermally fluctuate below T_c.

II. MATERIALS PREPARATION AND STRUCTURAL CHARACTERIZATION

Mn_3O_4 particles were chemically precipitated at room temperature by mixing $Mn(NO_3)_2$ aqueous solution and aqueous sodium hydroxide NaOH solution with pH$\sim$12. The obtained brown powder (manganese hydroxide) was washed with distillate water to remove the residual ions. The final solution was boiled in reflux during 5 days and a particle suspension was obtained. Powder sample of these particles (S1) was obtained by drying part of the suspension.

Diluted dispersions of Mn_3O_4 particles in a polyvinylpyrrolidone (PVP) aqueous solution were also prepared with 17.6% (sample S2) and 1.5% (sample S3) of particles in weight.

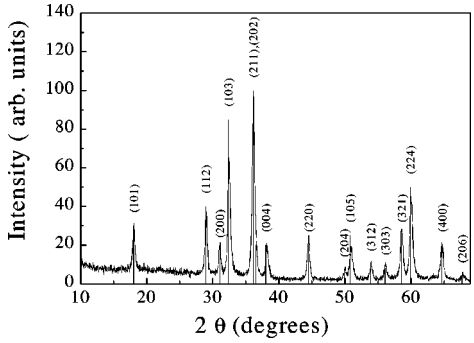

FIG. 1. X-ray (Cu K_α) diffraction pattern of Mn_3O_4 sample (S1).

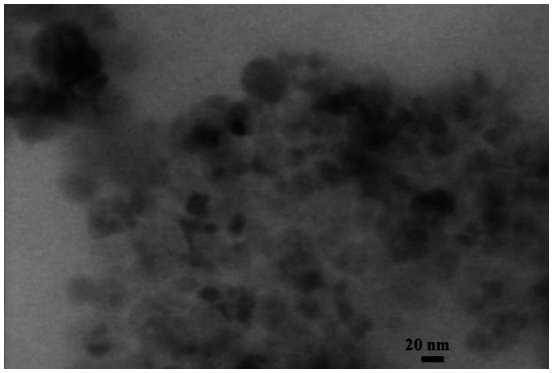

FIG. 2. TEM image of S1 sample (powder sample).

The x-ray diffraction pattern corresponds to the Mn_3O_4 phase, without any other phase (Fig. 1). The particle size distribution was determined by transmission electron microscopy (TEM) and light scattering experiments (Figs. 2 and 3). The TEM measurements were performed by a Philips CM200 UT instrument operating at 200 kV and the light scattering measurements by a commercial ZetaSizer 1000 apparatus working at 90° fixed angle.

The measured distribution is approximately log-normal with a mean diameter $\langle\phi\rangle = 15$ nm. Taking into account the concentration of the particle dispersions and the particle size, the interparticle distances were estimated in 40 nm and 100 nm for the 17.6% and 1.5% samples, respectively. In the S3 dispersed sample the particles are far enough to neglect dipole-dipole interactions and therefore the particles can be considered as non-interacting.

The magnetic properties were investigated in the 5–300 K temperature range in applied fields up to 5 T using a commercial SQUID magnetometer. The electron spin resonance (ESR) spectra were recorded by a Bruker ESP300 spectrometer at 9.5 GHz from room temperature down to 2 K.

III. RESULTS AND DISCUSSIONS

In Fig. 4, the results of magnetization measurement ($H = 50$ Oe) as a function of the temperature on S1, S2, and S3 samples are reported. The measurements were performed according to the usual zero field cooling (ZFC) and field cooling (FC) procedures. The magnetization increases going from S3 to S1 sample. With decreasing temperature, a rapid increase of the FC magnetization is observed for all the samples at $T_c = 42$ K, corresponding to the Curie temperature of bulk Mn_3O_4, accompanied by the appearance of magnetic irreversibility (difference between FC and ZFC curves). The transition temperature does not change with the applied field, as shown by the peak in the derivative of the FC magnetization vs temperature curve measured applying a field of 5 T (Fig. 5, inset). For the S3 sample, the application of 5 T determine a change of the M vs T curve towards a Curie-type behavior, reflecting the tendency of the particle moment to align in the field direction. The irreversibility (difference between FC and ZFC branches, Fig. 4) indicates an induced preferential orientation of the particle moments along the

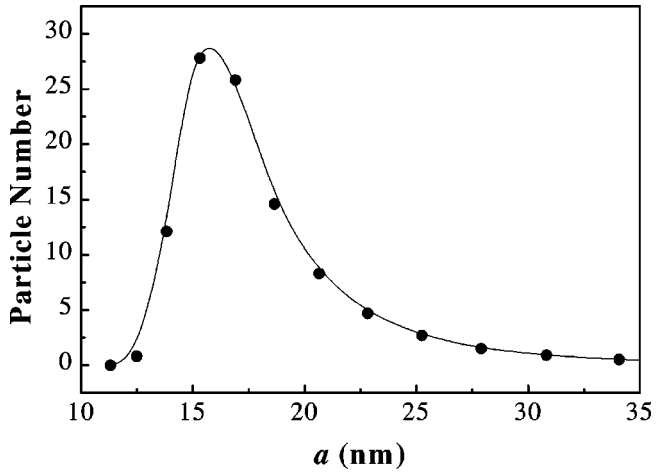

FIG. 3. Particle size distribution determinate by light scattering experiments.

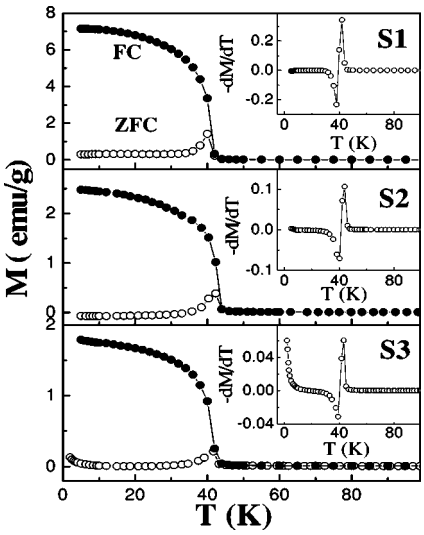

FIG. 4. Zero field cooled-ZFC (open circles) and field cooled since 100 K—FC (solid circles) magnetization measurements for samples S1, S2, and S3. The insets show the temperature derivative of the ZFC magnetization vs temperature.

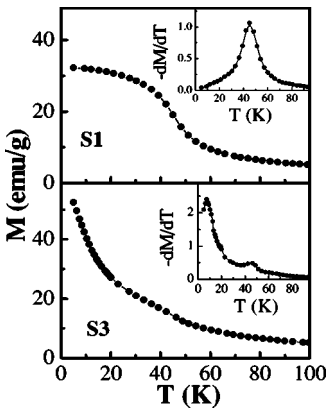

FIG. 5. Temperature dependence of the FC magnetization measured at 5 T for the S1 and S3 sample. The insets show the temperature derivative of the magnetization in function of the temperature.

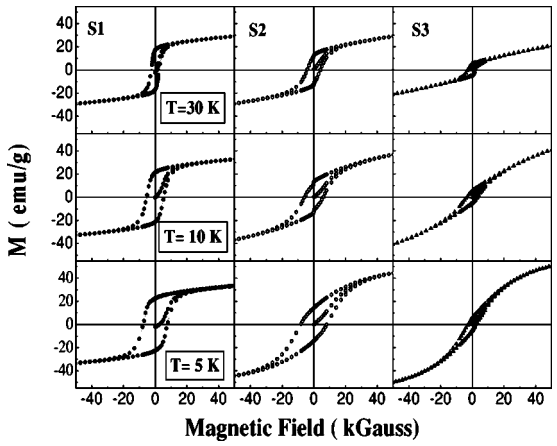

FIG. 6. Hysteresis loop of S1, S2, and S3 measured at $T=30$ K, 10 K, and 5 K.

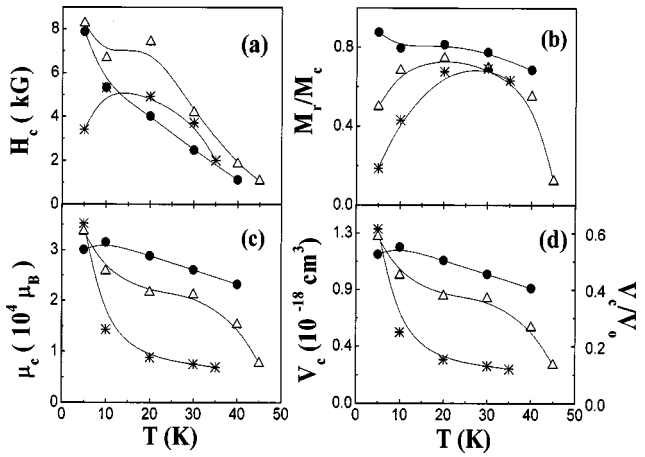

FIG. 7. Temperature dependence of (a) coercive field, (b) remanent magnetization normalize with the saturation magnetization, (c) and (d) magnetic moment and magnetically ordered volume of the nanoparticle, calculated from the extrapolation of the saturation magnetization at zero field, respectively. The fill circles correspond to S1, the open triangles correspond to S2, and stars correspond to S3.

applied field. No superparamagnetic behavior is observed, due to the high anisotropy of the material. Indeed the particle size is much larger than the superparamagnetic threshold volume (V_{th}) at $T=42$ K, $V_{\text{th}}=1.7\times10^{-19}$ cm^3 ($\phi_{\text{th}}=7$ nm), estimated from the Arrhenius law: $V_{\text{th}}=k_BT\log(\tau/\tau_0)/K$, where K is the anisotropy constant, (the anisotropy constant of bulk Mn_3O_4, $K_{\text{bulk}}\sim1\times10^6$ erg/cm^3, is taken[13]), k_B is the Boltzmann constant, τ is the measurement time (100 s), and τ_0 is the characteristic relaxation time (10^{-10} s is taken).

In the sample S3 (Fig. 4), consisting of noninteracting particles, a change of slope in the M vs T curve is observed at $T\sim7$ K, with a more rapid increase of magnetization, according to a Curie-type law, below this temperature. The derivative of the magnetization dM/dT shows a peak at this temperature (inset of Figs. 4 and 5).

In Fig. 6, magnetization as a function of magnetic field curves after ZFC for $T<T_c$ are reported. The observed behavior suggests the existence of two contributions to the magnetization: a saturating contribution, coming from the magnetically ordered particle core, and a nonsaturating one, up to a field of 5 T, coming from the structurally and magnetically disordered structure. The tendency to nonsaturation is more marked with decreasing interparticle interactions, i.e., going from S1 to S3 sample, for which an increase of the high field slope with decreasing temperature is observed. At low temperature, the cycles are not symmetrical with respect to the origin, showing a small shift towards negative fields (see Fig. 6). This effect has been also reported in bulk single crystals,[13] due to a realignment of ferromagnetic sublattices occurring at fields larger than 10 kOe. Hysteresis cycles were performed also after field cooling at the maximum field. No loop shift was observed, unlike what observed in other much smaller ferrimagnetic or antiferromagnetic nanoparticles systems, e.g., $NiFe_2O_4$ and NiO nanoparticles, respectively.[4,5] The absence of exchange bias effect is probably mainly due to the much lower surface/volume ratio in our particles.

In Fig. 7(a), the temperature dependence of the coercive field (H_c) is reported for the three samples. H_c values were extracted from the loops where the high field contribution of the magnetization was previously subtracted. It is noteworthy that for the S3 sample H_c shows a maximum at $\sim$20 K, we will discuss this point later. Moreover H_c of S2 sample is larger than the more dispersed one (S3) and decreases for the powder sample (S1) where the interactions are stronger. The H_c behavior observed for the three samples is due to the different degree of interparticles interactions. For S3, the interactions are negligible and the main contribution to H_c comes from the magnetocrystalline anisotropy; for S2, weak interparticle interactions (dipolar interaction) increase the effective anisotropy, leading to higher H_c values. For the powder sample, the interactions are much stronger and the exchange interactions lead to a decrease of the H_c value.[17]

In Fig. 7(b), the temperature dependence of the remanent magnetization M_r normalized to the core magnetization M_c, obtained by the extrapolation of the high field magnetization to $H=0$ is reported. For dispersed particle samples (S2 and S3), M_r/M_c shows a maximum centered at 20 K, whereas for the powder sample it is almost temperature independent. For the S3 sample, the low temperature decrease of both H_c and M_r/M_c reflects the narrowing of the hysteresis cycles at low temperature, as observed at 5 K (Fig. 6).

In Fig. 7(c), the corresponding temperature dependence of the particle core magnetic moment is reported. The particle core volume (on the right axis the core volume normalized to the total particle volume), was estimated from the particle core moment ($\mu_c=M_sV_c$) and is reported in Fig. 7(d). It is noteworthy that a large fraction of particle volume does not belong to the core and remains magnetically disordered. Moreover, the actual particle volume decreases going from the S1 to S3 sample and the volume of S3 increase when the temperature decreases, especially below 10 K. At 5 K, both the core volume and the particle moment have quite similar values for the three samples. The rapid increase of the core volume for S2 and S3 samples is in agreement with the decreasing of the free spins at the surface, due to the progressive freezing of magnetically ordered regions at the surface and the presence of interactions between surface and core

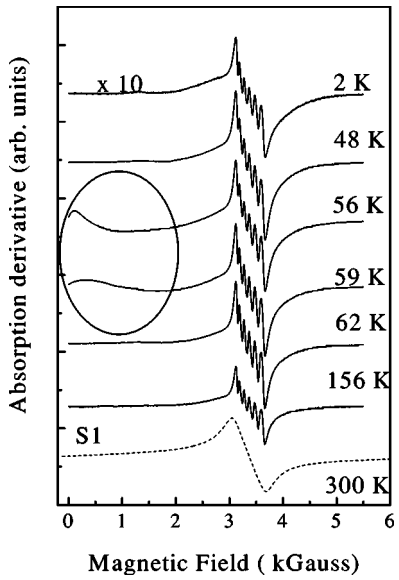

FIG. 8. *X*-band ESR spectra of S2 at different temperature and S1 at 300 K. The spectrum at $T=2$ K was reduced in a factor 10 in order to fit the same scale.

spins. This fact explains the approach of the core volume and magnetic moment of S2 and S3 samples to that of S1 sample at low temperature.

In Fig. 8, ESR spectra for the S2 sample at different temperatures and for the S1 sample at 300 K are reported. S3 sample has the same behaviour as S2 sample, but the spectra are weaker because of the smaller concentration of the particles in the polymer. The large line observed for the S1 sample corresponds to strongly interacting Mn^{+2} ions whose hyperfine spectrum is not resolved. When dipolar interactions between particles are present the ESR line is the result of the convolution of the spectra with different resonant fields due to the distribution of local effective fields. On the other hand, a hyperfine structure is observed in the spectrum of dispersed samples S2 and S3 (not shown). At 3300 Gauss the typical resonance of Mn^{+2} ions in the paramagnetic state is observed, superimposed to a large signal due to clusters of spins. The six lines correspond to the hyperfine splitting of the free spins due to the interaction between the electronic spin ($S=5/2$) and the nuclear spin ($I=5/2$). In this case it is able to observe the structure of the resonance line because the thermal fluctuations average to zero the dipolar interaction and, as a consequence, the linewidth of the resonance is shrunk. This behavior is usually found in compounds where the spins have high mobility, as in the case of Mn^{+2} ions in glasses or solutions. This result provides a clear evidence of the presence of free spins and cluster of spins, which should be located at the particle surface.

From Fig. 8 we also can see that at $T=59$ K, and for a few Kelvin, a ferromagnetic resonance line signal at low fields is observed. This resonance line is originated by the ferrimagnetically ordered core and it is observable only in a narrow range of temperature.[18,19] As mentioned above, due to the high anisotropy constant of Mn_3O_4, the ferromagnetic mode can be observed only in the short exchange interaction range from $T=59$ K to near T_c (we do not observe any change at T_c or below it). In the bulk sample, the short-range interaction is evidenced by the increase in the linewidth starting from $T=55$ K.[20]

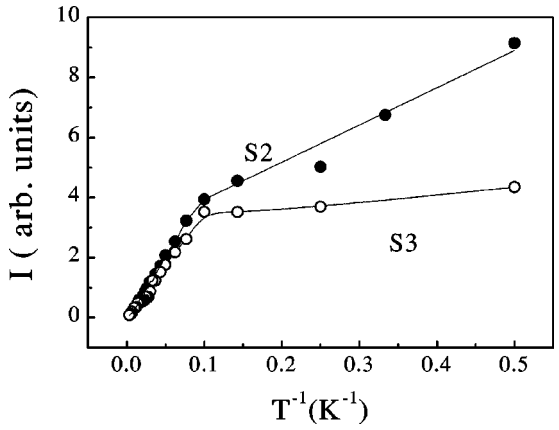

FIG. 9. Double integral of the paramagnetic ESR line as a function of the inverse temperature for S2 and S3 samples.

In Fig. 9, the double integral of the ESR lines (proportional to the magnetic susceptibility) with $g=2.020(5)$ is reported as a function of the inverse temperature, for the S2 and S3 samples. In order to compare both dependencies we have normalized the integral values (proportional to the magnetization) to the room temperature values. In both ESR *susceptibility curves* a change of the slope at $T=10$ K is observed. The curves present a smaller slope below 10 K, indicating a decrease of the free spins that may resonate with the microwave excitation. This is due to the slowing down of surface spin fluctuation, their subsequent freezing with decreasing temperature and the growth of exchange coupled clusters at the surface, interacting among them and with the core spins. The spin freezing is expected to be in random directions, according to the spin local atomic environments. The decrease of the slope in the S3 sample is much stronger than in the S2 sample. This indicates that the degree of surface disorder, associated with the fraction of free spins which freeze at low temperature, actually is higher in the more particle diluted sample.

The results of ESR experiments are coherent with those of magnetization measurements and allow us to gain a better insight into the comparison between the magnetic behavior of the three samples. The more rapid Curie-type increase of magnetization below 10 K, observed in the S3 sample, confirms the presence of a higher fraction of free spins at the particle surface with respect to the other two samples. Free surface spins are also responsible for the nonsaturation tendency in the M vs H curves, increasing with decreasing temperature. Consistently with the other experiments, the nonsaturation tendency is more marked going from the S1 to S3 sample, for which the free spins fraction is higher. These results are also in agreement with the observed maxima of both H_c and M_r/M_c for the S2 and S3 samples. Indeed, the low temperature decrease of both H_c and M_r/M_c is due to the increasing contribution to the magnetization with decreasing temperature from the paramagnetic (and superparamagnetic) component due to free spins and cluster spins. Moreover, the low temperature random spin freezing at the surface, tending

to demagnetize the sample, also contributes to the low temperature narrowing of the hysteresis cycles, reflected by the associated decrease of both H_c and M_r/M_c. The above results indicate a higher relative contribution to the total magnetization from the surface component with respect to the core component for the S3 sample consisting of noninteracting particles, as confirmed by the much smaller core magnetization and volume with respect to the other two samples.

IV. CONCLUSIONS

The magnetic properties of 15 nm Mn_3O_4 particle, in powder form (S1 sample) and dispersed in a polymer at different concentrations (17.6%, S2; 1.5%, S3) have been investigated by magnetization and ESR measurements. The S1 and S3 samples represent the two extreme cases of strongly interacting and noninteracting particles. The results provide evidence of a surface contribution to the observed magnetic properties, due to spins (and clusters of spins) which remain free to thermally fluctuate below the core ferrimagnetic temperature (T_c=42 K). The surface contribution manifests itself both in the magnetization (more rapid increase of the magnetization below 10 K and narrowing of the hysteresis cycle, for the S3 sample; non-saturation of the magnetization) and in the ESR (paramagnetic signal due to Mn^{+2} ions and cluster signal). With decreasing temperature, thermal spins fluctuations slow down, exchange coupled clusters grow and interact among them and with core spins and then a random freezing occurs at the surface according to the local environments. The observed surface effects decrease with increasing interparticle interactions.

Both magnetization and ESR measurements are coherent in providing evidence that the fraction of free spins at the surface decrease with increasing interparticle interactions (i.e., going from the S3 to the S1 sample) which actually prevent surface spins to thermally fluctuate. The phenomenon, observed for both dipole-dipole and exchange interactions, is more marked for the powder sample, where interparticle exchange interactions directly involve surface spins.

ACKNOWLEDGMENTS

This work has been accomplished with partial support by CONICET-CNR (Argentine-Italy) cooperation project and Fundación Antorchas (Argentine).

*Author to whom correspondence should be addressed. E-mail address: zysler@cab.cnea.gov.ar; Member of the Consejo Nacional de Investigaciones Científicas y Técnicas, Argentina.

[1] J.L. Dorman, D. Fiorani, and E. Tronc, Adv. Chem. Phys. **98**, 283 (1997).
[2] *Science and Technology of Nanostructurated Materials*, edited by G.C. Hadjipanayis and G.A. Prinz (Plenum, New York, 1991).
[3] R.W. Chantrell and K. O'Grady, *Applied Magnetism*, edited by R. Gerber *et al.* (Kluwer Academic, The Netherlands, 1994).
[4] R.H. Kodama, A.E. Berkovitz, E.J. McNiff, Jr., and S. Foner, Phys. Rev. Lett. **77**, 394 (1996).
[5] R.H. Kodama, Salah A. Makhlouf, and A.E. Berkovitz, Phys. Rev. Lett. **79**, 1393 (1997).
[6] R.H. Kodama and A.E. Berkovitz, Phys. Rev. B **59**, 6321 (1999), and references therein.
[7] H. Kachkachi, M. Noguès, E. Tronc, and D.A. Garanin, J. Magn. Magn. Mater. **221**, 158 (2000).
[8] O. Iglesias and A. Labarta, Phys. Rev. B **63**, 184416 (2001).
[9] E. De Biasi, C.A. Ramos, R.D. Zysler, and H. Romero, Phys. Rev. B **65**, 144416 (2002).
[10] R.D. Zysler, H. Romero, C.A. Ramos, E. De Biasi, and D. Fiorani, J. Magn. Magn. Mater. **266**, 233 (2003).
[11] Z. Weixin, W. Cheng, Z. Xiaoming, X. Zyi, and Q. Yitai, Solid State Ionics **117**, 331 (1999), and references therein.
[12] B. Boucher, R. Buhl, and M. Perrin, J. Appl. Phys. **42**, 1615 (1971).
[13] K. Dwight and N. Menyuk, Phys. Rev. **119**, 1470 (1960).
[14] G.B. Jensen and O.V. Nielsen, J. Phys. C **7**, 409 (1974).
[15] R. Metselaar, R.E. Van Tol, and P. Piercy, J. Solid State Chem. **38**, 335 (1981).
[16] I.S. Jacobs, J. Phys. Chem. Solids **11**, 1 (1959).
[17] R.D. Zysler, C.A. Ramos, E. De Biasi, H. Romero, A. Ortega, and D. Fiorani, J. Magn. Magn. Mater. **221**, 37 (2000).
[18] Yu.L. Raikher and V.I. Stepanov, Phys. Rev. B **50**, 6250 (1994).
[19] E. de Biasi, C.A. Ramos, and R.D. Zysler, J. Magn. Magn. Mater. **262**, 235 (2003); **278**, 289 (2004).
[20] G. Srinivasan and Mohindar S. Seehra, Phys. Rev. B **28**, 1 (1983).